J Mater Sci: Mater Med (2007) 18:441–447
DOI 10.1007/s10856-007-2003-3

Ion implantation modified stainless steel as a substrate for hydroxyapatite deposition. Part II. Biomimetic layer growth and characterization

L. Pramatarova · E. Pecheva · V. Krastev

Received: 11 July 2005 / Accepted: 14 November 2005

Abstract The interest in stainless steel as a material widely used in medicine and dentistry has stimulated extensive studies on improving its bone-bonding properties. AISI 316 stainless steel is modified by a sequential ion implantation of Ca and P ions (the basic ions of hydroxyapatite), and by Ca and P implantation and subsequent thermal treatment in air (600°C, 1 h). This paper investigates the ability of the as-modified surfaces to induce hydroxyapatite deposition by using a biomimetic approach, i.e. immersion in a supersaturated aqueous solution resembling the human blood plasma (the so-called simulated body fluid). We describe our experimental procedure and results, and discuss the physicochemical properties of the deposed hydroxyapatite on the modified stainless steel surfaces. It is shown that the implantation of a selected combination of ions followed by the applied methodology of the sample soaking in the simulated body fluid yield the growth of hydroxyapatite layers with composition and structure resembling those of the bone apatite. The grown layers are found suitable for studying the process of mineral formation in nature (biomineralization).

1 Introduction

It is found that metals form protective native oxide layer with a few nanometers thickness on their surfaces upon immersion in a supersaturated aqueous precursor solution (simulated body fluid, SBF) [1]. This oxide layer determines their excellent corrosion resistance and decreases the leaching of metal ions from the surface in the surrounding. The latter makes the metals appropriate for implantation in the human body, as well as the formation of an apatite layer (hydroxyapatite, HA) on their surfaces in the SBF, which is considered to ensure better bonding to bone [1]. After titanium, stainless steel is one of the most frequently used in medicine and dentistry areas metals due to its excellent corrosion resistance, mechanical properties and low cost.

Important in studying the process of mineral formation in nature (the so called biomineralization) is the study of the surface and its appropriate structural and/or chemical modification in such a way that to yield desired biological reactions and to improve the biomaterial performance, since they are subjected to different (aggressive) body fluids. Tailoring the surface through a definite technique is used for selective improvement of the material functions and effective lifetime by means of changing the physical, chemical, mechanical and other properties connected to the biocompatibility and functionality of the materials [2]. Ion implantation finds extensive application in biomaterials area for selective creation of functional surfaces with tailored biological activity [2]. This treatment improves the surface quality of metals in terms of surface hardness, wearing resistance, corrosion resistance, decrease of the friction, and etc. Other advantages of the technique are the increased surface hardness and the creation of passivating surface oxide layer on the surface of the metals which raise their native corrosion resistance in an aggressive medium [2–4]. The process can be applied on any material—metal, ceramic, polymer and etc., but its effects are specific for the particular material due to differences in the structure.

In last years, there is an increased interest in exploiting the possibilities of simple and cheap method of immersion the

L. Pramatarova · E. Pecheva (✉)
Institute of Solid State Physics, Bulgarian Academy of Sciences, 1784 Sofia, Bulgaria
e-mail: emily@issp.bas.bg

V. Krastev
Institute of General and Inorganic Chemistry, Bulgarian Academy of Sciences, 1113 Sofia, Bulgaria

materials in a supersaturated aqueous solution at low temperatures (<100°C). This solution known as SBF resembles the ion composition, concentrations and pH of the human blood plasma. This method is maximally approaching the conditions in nature at which minerals like HA are formed and is known as biomimetic approach [5, 6]. A preliminary mechanical or chemical modification of the material surface before its immersion in the SBF is usually carried out [7]. Thus, the opportunity for precipitation of homogeneous, dense and with a good adhesion calcium phosphate layers is higher. Other advantages are the possibility to obtain bio-like coating on materials with complex shapes and hence better implant connection with the bone, as well as the fact that the influence of high temperatures on the substrate required in some techniques is avoided. Although the increased number of studies, the exact mechanism by which coatings are produced with this method is not clear enough. The process of precipitation is complicated due to the chance for formation of few solid phases in dependence on the solution composition and its pH.

In this work AISI 316 stainless steel is modified by a sequential ion implantation of Ca and P ions (the basic ions of HA), and by Ca and P implantation and subsequent thermal treatment in air (600°C, 1 h) [7]. The ability of the as-modified surfaces to induce biologically like HA deposition by using the biomimetic approach is investigated.

2 Experimental details

2.1 Materials

Substrates with sizes of 8 mm × 8 mm × 1 mm are cut from AISI 316 stainless steel foil (Goodfellow, England). They are subjected to a standard procedure for cleaning, lapping and polishing, described in the first part of this paper [7]. Substrates prepared in this way are called initials and further in the text they are regarded as SS.

2.2 Ion implantation and thermal treatment

Sequential implantation of Ca and P ions is conducted to modify the whole surface of initial stainless steel samples. Applied doses, according preliminary theoretical calculations are in the range 7×10^{16}–2×10^{17} Ca ions/cm^{-2} and 5×10^{16}–8×10^{16} P ions/cm^{-2}. To reach an approximately homogeneous distribution, the implantation is conducted using three consecutive energy steps: 104, 92 and 80 keV for Ca ions and 61, 54 and 47 keV for P ions. After ion implantation, part of the samples is thermally treated at 600°C in air for 1 h to convert Ca and P to oxides. Further in the text, the ion-implanted samples and the thermally treated samples are denoted as SS0 and SS873, respectively.

2.3 Immersion in SBF

To evaluate the ability of the modified samples to precipitate HA, they are soaked in a SBF solution prepared according to Kokubo [6] and modified with 1.5 times higher Ca and P concentrations (Table 1). The solution is prepared by dissolving reagent-grade NaCl, $NaHCO_3$, KCl, K_2HPO_4-$3H_2O$, $MgCl_2$-$6H_2O$, $CaCl_2$-$6H_2O$, and Na_2SO_4-$10H_2O$ in distilled water, and buffered at pH 7.4 with tris-hydroxymethyl-aminomethane [$(CH_2OH)_3CNH_2$, TRIS] and hydrochloric acid (HCl). No precipitation is observed during the preparation. All samples studied are immersed simultaneously in 400 ml total volume of freshly prepared SBF for 108 h. The solution is kept in a water bath at a constant temperature of 37°C. Supersaturation conditions are maintained during the whole period of immersion of the samples. For this purpose 100 ml are removed from the solution and replaced by a fresh solution every 24 h. At the end of the immersion period the samples are washed gently with distilled water and dried in air.

2.4 Analyses

Scanning Electron Microscopy (SEM) images of the layer morphology are obtained using a Digital Scanning Electron Microscope DSM 962 (Carl Zeiss, Germany) operating at 15 kV. The elemental distribution in the layer is measured by Energy Dispersive X-ray (EDX) Spectroscopy (Norain, Voyager 1000). Transmission electron microscope (TEM) Philips CM300-SuperTWIN with operating voltage of 300 kV is also used in the study of the layer.

Surface and layer structure is investigated by Fourier Transform Infrared (FTIR), Raman spectroscopy and X-ray Diffraction (XRD). FTIR spectra are recorded in a reflection mode, spectral range of 4000–400 cm^{-1}, 100 scans, and resolution of 4 cm^{-1} by using Nikolet Magna IR 750 spectrometer. Raman spectra are acquired in a backscattering mode and Nd:YAG laser as a source (2ω, $\lambda = 532{,}14$ nm) on LabRam System 010, Jobin Yvon, with resolution of 3 cm^{-1}. XRD data are obtained at grazing incidence geometry (GIXRD) on XRD spectrometer with Cu$K_{\alpha 1}$ ($\lambda = 1, 54$ Å) X-ray source, scanning at $2\theta = 5 - 90^\circ$ with a step of $\Delta 2\theta = 0.01^\circ$ and measuring time 15 s at each position, operating voltage of 40 kV and operating current of 30 mA. JCPDS standard card 09-432 is used to identify the compound.

To estimate the adhesion strength of the layer to the surfaces, scratch test is carried out with a SST-101 Scanning Scratch Tester (Shimadzu, Japan). Ca and P concentrations in the SBF are measured every day by inductively coupled

Table 1 Ionic concentrations of SBF solutions, used by Kokubo and the authors, in comparison with the concentrations in human blood plasma

Concentration [mM]	Na^+	K^+	Mg^{2+}	Ca^{2+}	Cl^-	HCO_3^-	HPO_4^{2-}	SO_4^{2-}	pH
Blood plasma	142.0	5.0	1.5	2.5	103.0	27.0	1.0	0.5	7.4
Kokubo SBF [16]	142.0	5.0	1.5	2.5	147.8	4.2	1.5	0.5	7.25
SBF (1.5 times Ca,P)	142.0	5.0	1.5	3.75	147.8	4.2	1.0	0.5	7.4

plasma mass spectrometry (Elan 5000, Perkin Elmer) and ion chromatography (Metrohm).

3 Results and discussion

The ability of the modified surfaces to induce a layer precipitation is evaluated by soaking them into a supersaturated SBF for 108 h at physiological conditions (37°C and pH 7.4).

The morphology of the layers grown after 108 h, as well as the layer distribution on the modified by the ion implantation and by the thermal treatment surfaces are shown in Fig. 1. The SEM images show porous layer with different homogeneity, consisting of sphere-like clusters grouped in a porous network. The cluster sizes in the layers vary from very small to big, thus leading to an average diameter of 2–3 μm.

Ion implanted stainless steel samples (SS0, Fig. 1b) induce the most homogeneous and dense layer. As discussed in [7], the results of the XPS and AES confirm the incorporation of the implanted Ca and P in the steel matrix, and thus the ions are considered to play the role of surface nuclei which facilitate the easier growth of layer from the SBF by efficient adsorption of Ca^{2+} and PO_4^{2-} ions on the SS0 surfaces thereby inducing more uniform and dense layer. The most inhomogeneous layer is observed on the control samples (SS, Fig. 1a). The thermally treated after the implantation samples also induce the precipitation of inhomogeneous layer (SS873, Fig. 1c). It is generally accepted that metal oxides charge the surface negatively in an aqueous environment due to amphoteric OH^- groups and this could be advantageous to the induction of HA precipitation from the SBF [8]. However, to say unambiguously what is the effect of the surface modifications on the layer growth, we should observe its morphology in an early stage of the process of growth.

The elemental composition of the layers is measured by EDX on at least four squared areas with sizes 10×10 μm situated on different places on the sample surface. Except the signals of Fe and Cr coming from the stainless steel substrate, EDX spectroscopy shows the presence of Ca, P, O and C in all spectra (Fig. 2a–c). The predominant elements in the layers on the surface of SS0 and SS873 samples are Ca and P (Figs. 2b and c), whose concentration is much higher than that in the layer grown on SS samples (Fig. 2a). Traces of Na and Mg are also observed in the layers, which means that these elements are incorporated in the layer structure during its growth from the SBF. By using EDX it is also possible to determine the ratio Ca to P that shows which CaP phase is formed. For example, Ca: P = 1.67 corresponds to stoichiometric HA (s-HA), lower value shows incorporation of foreign elements and/or formation of other calcium phosphate phases differing from s-HA [9]. The Ca:P ratio calculated in our experiment shows higher value for the ion implanted

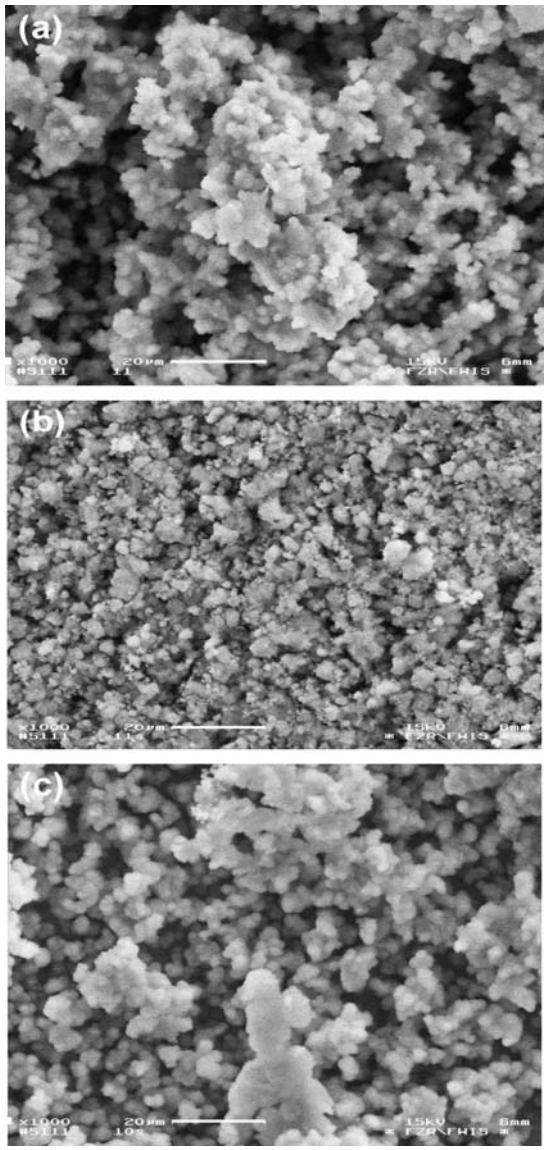

Fig. 1 Morphology of the layers grown on SS, SS0 and SS873 samples (bar 20 μm).

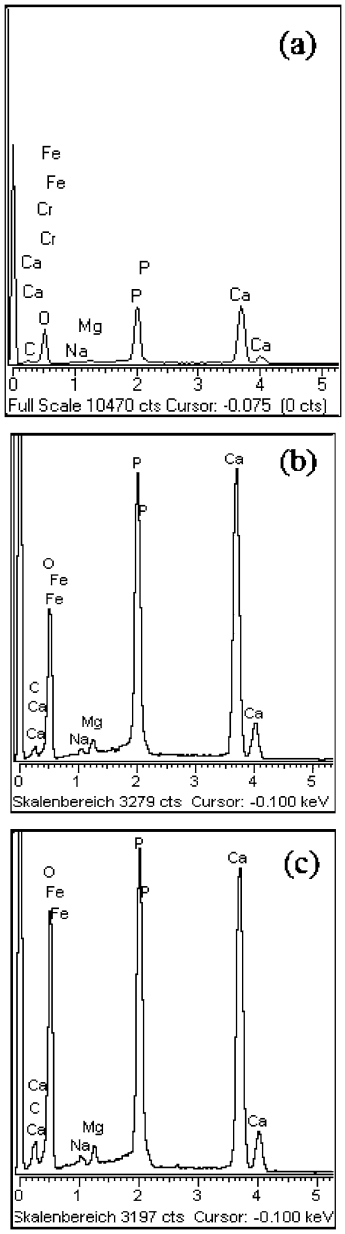

Fig. 2 EDX spectra show the elemental composition in the layers grown on SS, SS0 and SS873 samples.

steel samples (1.41), followed by the thermally treated samples (1.36) and the initials (1.30).

The layer precipitated on the ion implanted samples is observed also by TEM. Figure 3 shows the images of the layer and the stainless steel substrate. It can be seen that the layer consists of fine needle-like crystals. The corresponding diffraction pattern (inset 1) shows a crystallographic fraction characterized by a uniform spacing of about 0.27 nm, which corresponds to HA according to the standards for identification. According to them, the HA strongest reflection is associated with a spacing of 0.2814 nm (JCPDS card 09-432). It is known that a diffused halo is obtained when the layer is

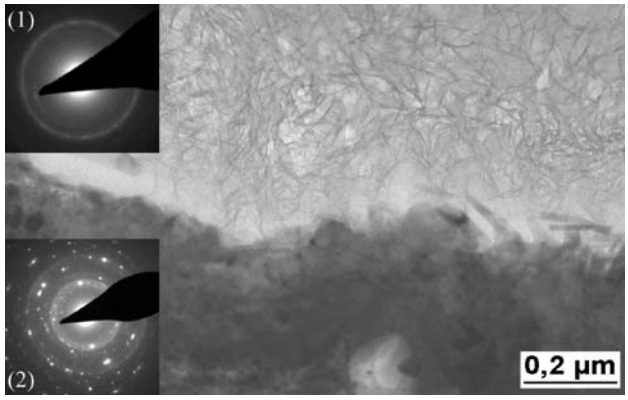

Fig. 3 TEM image of the layer grown on SS0 samples (up) and of the ion implanted substrate (down). Insets (1 and 2) show the corresponding diffraction patterns.

amorphous or it consists of many small crystals (<100 nm in size) without a preferential orientation. XRD measurements carried out in parallel show that the layers are not completely crystalline, show no preferential orientation, and the crystal grain size is in the order of 36 nm (in correspondence with the TEM images). The diffraction pattern of the substrate (down left) is typical for a polycrystalline material like the stainless steel.

In accordance to the standards, GIXRD patterns (Fig. 4) clearly show the formation of HA by the presence of the strong (002) peak at $2\theta = 25.9^\circ$, as well as by (211), (112), (300) and (202) peaks, situated under the broad and intensive contour centered at 32.2°. Because of the fact that these peaks situated at $2\theta = 31.8^\circ, 32.2^\circ, 32.9^\circ$ and 34.1° are overlapped it is concluded that the layer is not fully crystalline. The isolated (002) peak is used to calculate the crystal grain size by using Scherrer's equation [10]. Calculated values of 34 for the thermally treated after the implantation and 38 nm for the initial samples correspond well to the size of the bone mineral apatite crystals, which are known to be relatively small, i.e. in the range of 20–40 nm [11]. The larger grain size of the HA grown on initial steel samples (SS, grain size 38 nm) indicate higher crystallinity in comparison to the layer grown on the corresponding modified samples (SS873, grain size 34 nm) [12]. Besides the HA characteristic peaks, two peaks of austenite iron at 43.7° and 50.8° are clearly observed in the case of the spectra of the HA on the SS samples which induce the growth of a layer with lower thickness as shown by the lower intensity of the characteristic HA peaks in SS+HA spectrum in Fig. 4.

FTIR absorption spectra are recorded on the stainless steel samples before and after their immersion in the SBF. The spectra of the samples after ion implantation, after thermal treatment and initials do not show any absorption band (spectra not presented). FTIR measurement of the layers grown after the samples soaking in the SBF (Fig. 5a) support the XRD results for the formation of HA by showing absorption

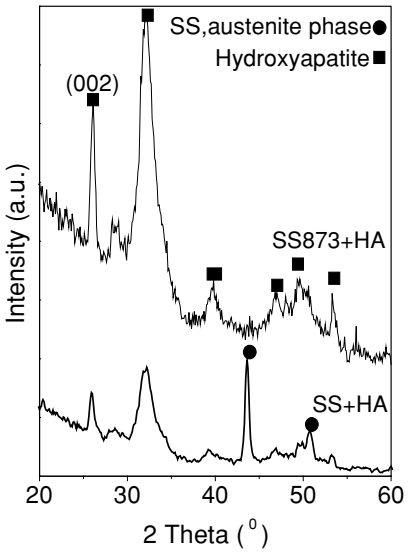

Fig. 4 XRD spectra of the HA layer grown on the SS873 samples, compared to initials (SS) after their soaking in SBF.

from PO_4^{3-} groups at 560 and 600 cm^{-1} (ν_4 bending), and 980–1110 cm^{-1} (ν_1 and ν_3 stretching region), typical for HA. The spectra reveal also incorporation of CO_3^{2-} groups into the apatite structure by a band at 872 cm^{-1} (ν_2 bending) and a weak peak splitting at 1420/1460 cm^{-1} (ν_3 stretching), and also of HPO_4^{2-} ions by a peak at 530 cm^{-1}. It is known that HPO_4^{2-} ions show absorption also at 875 cm^{-1} which coincides in these spectra with the absorption of CO_3^{2-} groups [9, 13]. CO_3^{2-} ions are found in carbonate apatite, the bone-like apatite, and the presence of HPO_4^{2-} ions is typical for octacalcium phosphate (OCP). Both ions are known to decrease the crystallinity of HA [9]. We consider that the observed by XPS phosphates (OCP and dicalciumphosphate dihydrate, DCPD) obtained as a result of the ion implantation serve as stimuli for the preferential and intermediate (i.e. without a precursor phase as amorphous calcium phosphate) growth of HA. It is known that DCPD and OCP are often present as intermediate phases during precipitation of the thermodynamically more stable HA [13]. It should be also mentioned that OCP has a great structural similarity to HA and might serve as a template for epitaxial growth of HA [9, 14]. Typical for the FTIR spectra of HA is the presence of OH^- groups. Narrow absorption peak at 1654 cm^{-1} and a very broad peak starting from 2900 to 3700 cm^{-1} (not presented) are observed in the spectra of stainless steel samples (modified and initials, Fig. 5a). These are ascribed to O-H bending and O-H stretching vibrations of OH groups. Based on the FTIR results we consider that part of the OH groups is substituted by CO_3 groups, as it is known that the apatite structure is very tolerant of ionic substitutions [9, 15].

To evaluate the crystallinity of the layers grown on the three groups of samples (SS, SS0 and SS873), peak fitting is applied to the ν_4 phosphate region (Fig. 5b). It is easier to make peak fitting in the chosen region due to the low number of peaks situated under a common contour. The intensity ratio of 600 to 560 absorption bands ($I_{600} : I_{560}$) is used as an index of the crystal size perfection and it increases as crystallinity improves [16]. The calculated ratio for SS+HA, SS0+HA and SS873+HA samples of 1.4, 1.0 and 0.9, respectively, show higher crystallinity of the HA grown on the initial samples and the lowest layer crystallinity on the thermally treated samples. These results correlate well with the grain size estimation made by XRD.

Raman spectroscopy is known as a method that gives clear-cut information for the structure of inorganic compounds like HA. Using this method one can obtain information from the frequency region of 100–300 cm^{-1} which shows vibrational modes strongly specific for the crystal structure. Due to the fact that Raman spectroscopy and FTIR successfully complement each other, they are both used in this experiment.

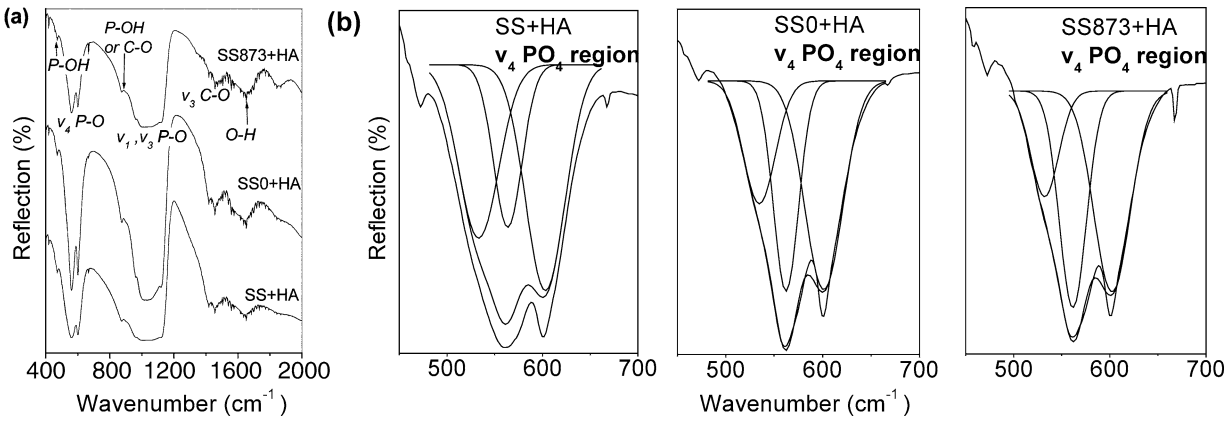

Fig. 5 (a) FTIR spectra of the layer grown on the surfaces of SS, SS0 and SS873 samples after their soaking in SBF; (b) peak fitting results in the ν_4PO_4 region allows to evaluate the crystallinity of the CO_3-containing HA layer through the ratio of $I_{600} : I_{560}$.

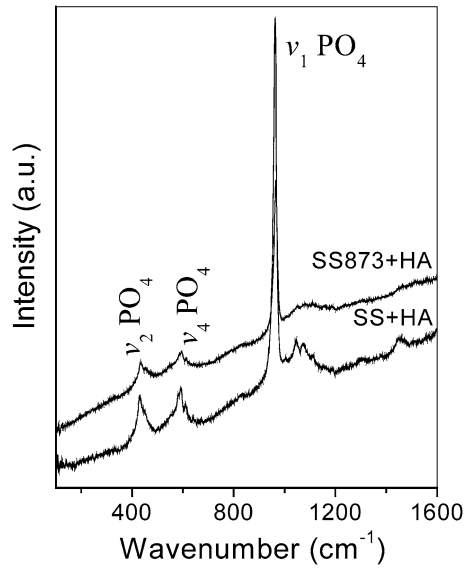

Fig. 6 Raman spectra of the HA layer grown on the modified stainless steel samples (SS0 and SS873, compared to initials) after their soaking in SBF.

Typical for HA peaks are observed in the Raman spectra of the layers grown on the modified steel samples after their soaking in the SBF (Fig. 6). Strong $\nu_1 PO_4$ symmetric stretching at 965 cm^{-1}, and three groups of peaks situated under common envelope and corresponding to ν_2 (433, 450 cm^{-1}), ν_4 (592, 614 cm^{-1}) and ν_3 (1044, 1072 cm^{-1}) PO_4 vibrational modes are detected in the spectra.

The results obtained by EDX and FTIR spectroscopy show low Ca:P ratio (lower than 1.67, the ratio for s-HA) which is typical for apatites grown by biomimetic method as in our experiment. This is due to the fact that some of the PO_4^{3-} and/or OH^- groups in the HA structure have been substituted by CO_3^{2-} groups (the property of the apatite structure to be tolerant of ionic substitutions [9, 15]). Bone has a complex composition, it contains CaP, HPO_4^{2-}, CO_3^{2-}, Mg, Na, K, F, Si and other elements in minor concentrations, some of them often preventing and others stimulating the formation of s-HA [9, 11, 17]. FTIR spectroscopy shows the presence of CO_3, HPO_4 and OH groups, and EDX shows the incorporation of Mg and Na ions in the layer. It can be summarized that the grown layer on the modified and initial samples is CO_3-containing HA with incorporation of CO_3^{2-}, HPO_4^{2-}, Mg and Na. It is known that non-stoichiometric apatites containing both CO_3^{2-} and HPO_4^{2-} ions are characterized by higher dissolution as biological apatite. Thus, the grown in this experiment HA layer mimic the bone apatite not only in the way it has been grown (from a supersaturated aqueous solution—a biomimetic approach) but also in structure and composition, and therefore it is suitable for studying the process of biomineralization.

In addition to the microscopic and spectroscopic methods for characterization of the layer, scratch test is performed to check the adhesion of the grown HA layer to the substrates. The adherence of the overgrown HA layers to stainless steel, modified by ion implantation, thermal treatment and initial samples is low; the layers could be peeled off by scrapping. However, observations with optical microscope show that at peeling off the layers with a scalpel, the blade reaches a very thin layer on all surfaces, which can not be detached. This result means that an initial thin layer with a significant adhesion to the surface of the three groups of samples is formed. The reason for the measured low adhesion is ascribed to a low cohesion between the clusters forming the overgrown layers under mechanical testing [18].

4 Conclusions

The whole surface of AISI 316 stainless steel has been modified by a sequential Ca and P ion implantation, as well as by Ca and P implantation and subsequent thermal treatment in air. The bioactivity of the modified surfaces is examined through the growth of HA layer from a supersaturated SBF at physiological conditions.

The grown layers consist of sphere-like clusters grouped in a porous network. The average cluster diameter is 2–3 μm. TEM results reveal that the layer consists of fine needle-like crystals identified by XRD as HA. Ion implanted samples induce the most homogeneous and dense layer, which is assigned to the introduction of Ca and P nuclei on the surface with the ion implantation. The most inhomogeneous layer is observed on the control samples. The thermally treated after the implantation samples also induce the precipitation of inhomogeneous layer. The layer formation on these samples is ascribed to the negative charge that metal oxides induce on surfaces in an aqueous environment due to OH^- groups. However, to say unambiguously what is the effect of the surface modifications on the layer growth, its morphology should be observed in an early stage of the growth process. The layer-surface adhesion is significant, but the cohesion between the clusters forming the overgrown HA layers is low.

The elemental composition of the layers consists of Ca, P and O, whose concentration is much higher than that in the layer grown on the initial surfaces. The presence of small amounts of Mg and Na in the spectra shows that they are incorporated into the layer structure. The calculated Ca:P ratio shows higher value for the ion implanted steel samples, followed by the thermally treated and the initial samples.

The layer is not completely crystalline and has no preferential orientation. Analysis show higher crystallinity of the HA grown on the initial samples, followed by the ion implanted steel, and the lowest layer crystallinity is obtained on the thermally treated samples. The calculated average grain

size is 36 nm, in correspondence with the TEM image and with the size of the bone mineral apatite crystals. FTIR and Raman spectroscopy reveal that the grown layer is CO_3^{2-} and HPO_4^{2-}-containing HA and we consider a substitution of some of the PO_4^{3-} and/or OH^- groups in the HA structure by CO_3^{2-} and HPO_4^{2-} groups.

It can be summarized that the grown in this experiment HA layer mimic the bone apatite not only in the way it has been grown, i.e. by applying a biomimetic approach, but also in morphology, structure and composition, and therefore it is suitable for studying the process of biomineralization.

Acknowledgments We would like to thank our colleagues Dr. M. F. Maitz, Dr. M. T. Pham, as well as E. Christalle for SEM/EDX and K. Fukarek for scratch test measurements. This research was supported by a Marie Curie grant No HPMT-CT-2000-00182 of the European Community and in part, by the Bulgarian National Scientific Research Fund through Grant L1213/2002.

References

1. M. UCHIDA, H. KIM, F. MIYAJI, T. KOKUBO and T. NAKAMURA, *Biomaterials* **23** (2002) 313.
2. P. SIOSHANSI and E. TOBIN, *Surf. Coat. Technol.* **83** (1996) 175.
3. W. LACEFIELD, Materials characteristics of uncoated/ceramic-coated implant materials, Presented at the 15th International Conference on Oral Biology (ICOB), Oral Biology and 4. Dental Implants, Baveno, Italy, June 28–July 1, (1998).
4. P. SIOSHANSI, *Nucl. Instrum. Meth. B* **24–25** (1987) 767.
5. A. CAMPBELL, G. FRYXELL, J. LINEHAN and G. GRAFF, *J. Biomed. Mater. Res.* **32** (1996) 111.
6. T. KOKUBO, H. KUSHITANI, S. SAKKA, T. KITSUGI and T. YAMAMURO, *J. Biomed. Mater. Res.* **24** (1990) 721.
7. L. PRAMATAROVA, E. PECHEVA, V. KRASTEV and F. RIESZ, *J. Mater. Sci.: Mater. Med.* **X** (2006) XXX.
8. H. WEN, J. WIJN, Q. LIU, K. DE GROOT and F. CUI, *J. Mater. Sci.: Mater. Med.* **8** (1997) 765.
9. J. ELLIOT, in "Structure and Chemistry of Apatites and Other Calcium Orthophosphates" (Elsevier Science B.V., Amsterdam, 1994).
10. B. CULLITY, in "Elements of X-ray diffraction" (Addison-Wesley Publishing Company Inc., Reading, Ma., 1956) p. 97.
11. A. BOSKEY, in "Dynamics of bone and cartilage metabolism" edited by M. SEIBEL, S. ROBINS and J. BILEZIKIAN (Academic Press, 1999) p. 153.
12. S. GADALETA, E. PASCHALIS, F. BETTS, R. MENDELSOHN and A. BOSKEY, *Calcif. Tissue Int.* **58** (1996) 9.
13. R. LeGEROS and J. LeGEROS, in "Phosphate minerals in human tissues. In Phosphate Minerals" edited by J. NRIAGU and P. MOORE (Springer Verlag, New York, 1984) p. 351.
14. W. BROWN, J. SMITH, J. LEHR and A. FRAZIER, *Nature* **196** (1962) 1048.
15. H. BENHAYOUNE, D. CHARLIER, E. JALLOT, P. LAQUERRIERE, G. BALOSSIER and P. BONHOMME, *J. Phys. D: Appl. Phys.* **34** (2001) 141.
16. L. MILLER, V. VAIRAVAMURTHY, M. CHANCE, R. MENDELSOHN, E. PASCHALIS, F. BETTS and A. BOSKEY, *Biochim. Biophys. Acta.* **1527** (2001) 11.
17. E. JALLOT, *Appl. Surf. Sci.* **211**(1–4) (2003) 89.
18. J. ARIAS, M. MAYOR, J. POU, Y. LENG, B. LEON and M. PEREZ-AMOR, *Biomaterials* **24** (2003) 3403.